02

Classification of Human Carotid Atherosclerotic Lesions With In Vivo Multicontrast Magnetic Resonance Imaging

Jian-Ming Cai, MD, PhD; Thomas S. Hatsukami, MD; Marina S. Ferguson, BS; Randy Small, BS; Nayak L. Polissar, PhD; Chun Yuan, PhD

Background—Recent studies demonstrated that in vivo and ex vivo MRI can characterize the components of the carotid atherosclerotic plaque, such as fibrous tissue, lipid/necrotic core, calcium, hemorrhage, and thrombus. The purpose of this study was to determine whether in vivo high-resolution multicontrast MRI could accurately classify human carotid atherosclerotic plaque according to the American Heart Association classification.

Methods and Results—Sixty consecutive patients (mean age 70 years; 54 males) scheduled for carotid endarterectomy were imaged with a 1.5-T scanner after informed consent was obtained. A standardized protocol was used to obtain 4 different contrast-weighted images (time of flight and T1-, PD-, and T2-weighted) of the carotid arteries. Best voxel size was $0.25\times0.25\times1$ mm^3. Carotid plaques were removed intact and processed for histological examination. Both MR images and histological sections were independently reviewed, categorized, and compared. Overall, the classification obtained by MRI and the American Heart Association classifications showed good agreement, with Cohen's κ (95% CI) of 0.74 (0.67 to 0.82) and weighted κ of 0.79. The sensitivity and specificity, respectively, of MRI classification were as follows: type I-II lesions, 67% and 100%; type III lesions, 81% and 98%; type IV-V lesions, 84% and 90%; type VI lesions, 82% and 91%; type VII lesions, 80% and 94%; and type VIII lesions, 56% and 100%.

Conclusions—In vivo high-resolution multicontrast MRI is capable of classifying intermediate to advanced atherosclerotic lesions in the human carotid artery and is also capable of distinguishing advanced lesions from early and intermediate atherosclerotic plaque. (*Circulation.* 2002;106:1368-1373.)

Key Words: magnetic resonance imaging ■ atherosclerosis ■ carotid arteries

Atherosclerosis is a chronic disease that affects medium and large arteries. The resultant plaque may grow to obstruct the lumen or to disseminate material into the blood stream and may cause myocardial infarction, stroke, and peripheral vascular disease.[1-3] In an attempt to categorize these complex lesions, the American Heart Association (AHA) created a detailed classification scheme that is designed to be used as a histological "template" for images obtained by a variety of invasive and noninvasive techniques in the clinical setting.[1-4] Accurate tracking of lesion types in vivo would be very useful clinically to determine the status of atherosclerosis.

See p ●●●

A number of recent publications[5-12] demonstrated that in vivo and ex vivo MRI can characterize the composition of human carotid atherosclerotic plaque, such as fibrous tissue, lipid and necrotic core, calcium, hemorrhage, thrombus, and the status of the fibrous cap (FC). Shinnar and colleagues[6] showed that by using multiple MRI sequences and images, atherosclerotic plaques could be completely characterized with high sensitivity and specificity ex vivo. Yuan et al[8] demonstrated that in vivo multispectral MRI could identify the lipid-rich necrotic core and recent intraplaque hemorrhage in human carotid atherosclerosis with high sensitivity and specificity. Because lesion types are fundamentally based on the various components of the plaque, multicontrast-weighted MRI is crucial for lesion-type classification. The purpose of the present study was to test the hypothesis that in vivo multicontrast-weighted MRI could accurately classify human carotid atherosclerotic plaques according to a modified histological classification scheme based on AHA guidelines.

Methods

Study Population

Between September 1998 and March 2001, 60 consecutive patients (mean age 70 years; 54 males) scheduled for carotid endarterectomy at the University of Washington Medical Center or VA Puget Sound Health Care System were recruited for the study after informed consent had been obtained. Institutional review boards of each

Received April 3, 2002; revision received June 14, 2002; accepted June 17, 2002.

From Department of Radiology (J.-M.C., M.S.F., R.S., C.Y.), University of Washington, Seattle, Wash; Department of Radiology (J.-M.C.), PLA General Hospital, Beijing, China; Surgical Service (T.S.H.), VA Puget Sound Health Care System, Seattle, Wash; and Mountain-Whisper-Light Statistical Consulting (N.L.P.), Seattle, Wash.

Correspondence to Dr Chun Yuan, Department of Radiology, University of Washington, Box 357115, Seattle, WA 98195-7115. E-mail cyuan@u.washington.edu

Circulation is available at http://www.circulationaha.org

DOI: 10.1161/01.CIR.0000028591.44554.F9

TABLE 1. Conventional and Modified AHA Classification of Atherosclerotic Plaque

Conventional AHA Classification	Modified AHA Classification for MRI
Type I: initial lesion with foam cells	Type I–II: near-normal wall thickness, no calcification
Type II: fatty streak with multiple foam cell layers	
Type III: preatheroma with extracellular lipid pools	Type III: diffuse intimal thickening or small eccentric plaque with no calcification
Type IV: atheroma with a confluent extracellular lipid core	Type IV–V: plaque with a lipid or necrotic core surrounded by fibrous tissue with possible calcification
Type V: fibroatheroma	
Type VI: complex plaque with possible surface defect, hemorrhage, or thrombus	Type VI: complex plaque with possible surface defect, hemorrhage, or thrombus
Type VII: calcified plaque	Type VII: calcified plaque
Type VIII: fibrotic plaque without lipid core	Type VIII: fibrotic plaque without lipid core and with possible small calcifications

facility approved the consent forms and study protocols. All patients underwent a carotid artery MRI examination within 1 week of the surgical procedure. The specimens were fixed in formalin, decalcified, and embedded in paraffin. Samples were sectioned (10 μm thick) every 0.5 to 1.0 mm throughout the length of the endarterectomy specimen and stained (hematoxylin-eosin and Mallory's trichrome). An established protocol was used for the histology processing, which is documented in Yuan et al.[8]

MRI Protocol

Patients were imaged with a custom-designed phased-array carotid coil in a 1.5-T GE Signa scanner (Horizon EchoSpeed, version 5.6/5.8, GE Medical Systems). A standardized protocol was used to obtain 4 different contrast-weighted images (time of flight [TOF] and T1-, PD- and T2-weighted) of the carotid arteries 2 cm proximal and 2 cm distal to the bifurcation.[8] Fat suppression was used to reduce signal from subcutaneous fatty tissues. Parameters for the imaging sequences were as follows: (1) double-inversion recovery T1-weighted 2D fast spin-echo (repetition time [TR]/TI/time to echo [TE] 800/650/9.3 ms, field of view [FOV] 13 cm, thickness 2 mm, 256×256 matrix, number of excitations [NEX] 2), (2) cardiac-gated, shared echo fast spin-echo for PD-weighted and T2-weighted images (TR 3RR, first echo TE 20 ms, second echo TE 40 ms, FOV 13 cm, thickness 2 mm, 256×256 matrix, NEX 2); and (3) 3D-TOF (TR/TE 23/3.8 ms, flip angle 25°, FOV 13 cm, thickness 1 to 2 mm, 256×256 matrix, NEX 2). With zero-padded Fourier transform, the best voxel size achieved was $0.25\times0.25\times1.0$ mm^3.

Image Review

Per-artery based image-quality rating (5-point scale, 1=worst, 5=best) for each contrast weighting was assigned to all MR images[8] before the review. For each imaging location, there were 4 images available to be reviewed to determine the lesion type. To decrease dependence on lesion type, images were selected at 4-mm distances. This protocol generated 4 to 6 image locations per artery that could be compared with histological sections of the endarterectomy specimens. All MR images from each of the contrast weightings were filmed and examined by one radiologist (J.-M.C.) who was blinded to the histological findings. The histology slides were reviewed independently by a reviewer (M.S.F.) who was unaware of the imaging results and were categorized according to the AHA classification (Table 1) based on the histopathological classification described by Stary et al.[1,4]

Our modified lesion-type classification scheme (Table 1) was derived from experience reviewing MR images and an extensive literature review of atherosclerosis publications.[1,3–8,12] In this classification scheme, types I and II of the AHA classification were combined into type I-II. The current resolution of MRI does not allow for the differentiation of discrete foam cells in type I and the multiple foam cell layers of the fatty streak in type II. Types IV and V in the AHA classification were combined into type IV-V because the ability of MRI to distinguish the proteoglycan composition of the type IV cap versus the dense collagen of the type V cap has not been demonstrated.

The imaging features used to identify these lesion types were as follows: FC, calcification, lipid or necrotic core, hemorrhage, and fibrosis. Given the current level of resolution by MRI, types I and II are indistinguishable from the near-normal carotid wall. Histologically, type III is characterized by a slight diffuse or eccentric thickening of the wall containing pools of extracellular lipid. In T1WI and PDWI, these pools appeared as focal, slightly high signals in some cases. Histologically, type IV-V contains a lipid or necrotic core, which by MR may have high signal intensity (SI) or iso-SI on T1WI, high or iso-SI on PDWI, and varied SI on T2WI. Interpretation of SI was made with reference to the immediately adjacent sternocleidomastoid muscle.[8]

The lumen surface defect and recent hemorrhage in type VI can be detected by multicontrast MRI.[8,12,13] The intact and thick FC (>0.25 mm) appears as a juxtaluminal band of low signal in TOF images. The absence of this hypointense band indicates the possibility of a thin, absent, or remodeling cap. A rupture is suspected when the band is absent on TOF and a region of high SI is adjacent to the lumen.[12] Recent hemorrhage appears as high SI in both T1WI and TOF images.[13] The extended calcification of the type VII plaque is readily detected by MRI, showing irregular low SI on all contrast-weighted images. Type VIII is a highly fibrotic lesion that often displays moderate to severe stenosis and is classified as such when the criteria for types IV-V, VI, and VII are excluded.

Correlation Between MRI and Histology

MR images and histological sections were independently reviewed and categorized. The process of matching images to histology sections used landmarks such as the relative distance from the common carotid bifurcation and gross morphological features such as lumen size and shape, as well as calcifications. Shrinkage of the specimens due to processing is very inconsistent throughout the specimen, and multiple aids in landmarks are required for accurate matching.[8]

Data Analysis

Cohen's κ with 95% CI, sensitivity, and specificity were determined with SPSS for Windows (version 10). Cohen's κ and weighted κ were computed to quantify the agreement between the MRI findings and histology. For weighted κ, full weight was given to perfect agreement, half weight was given to disagreement by 1 grade, and zero weight was given to other disagreements. A κ value of 0.61 to 0.80 indicates good agreement, and 0.81 to 1.0 indicates very good agreement.[14]

Because multiple image locations from each patient were used for statistical evaluation, the lesion types obtained from adjacent locations were assessed for interdependence by comparison of the MRI classification of each location with the classification of the next distal location ("forward" κ) and calculation of Cohen's κ. A similar comparison was made for each location and the next proximal location ("backward" κ).

Results

One endarterectomy specimen was unsuitable for histology analysis because of disruption during histological processing, and 7 patients were excluded because of an image quality of ≤2 caused by patient motion during the scan. The remaining 52 patients provided 252 locations (average 5 locations per

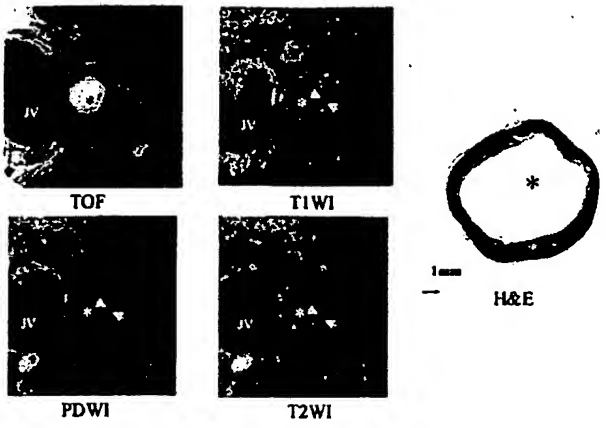

Figure 1. Example of type I-II lesion in common carotid artery (layered foam cells were detected by histology). On multicontrast-weighted MR images, carotid wall appears normal (arrow). * indicates lumen; JV, jugular vein; H&E, hematoxylin and eosin. Original magnification ×10.

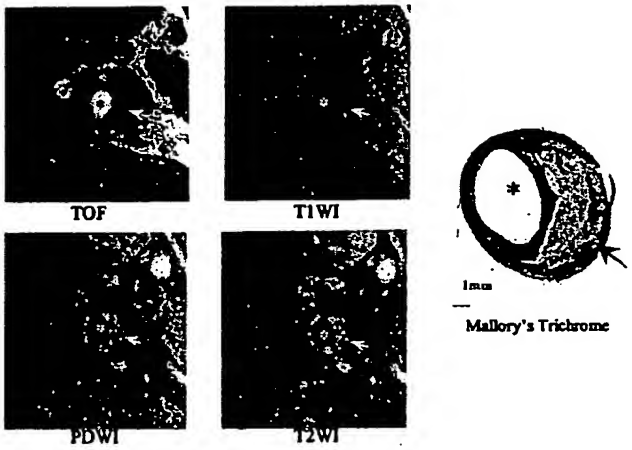

Figure 3. Example of type IV-V lesion in internal carotid artery (lipid-rich necrotic core was detected by histology). On multicontrast-weighted MR images, lipid-rich necrotic core (arrow) had iso-SI on both T1WI and TOF images, but iso-SI to slightly high SI on PDWI and T2WI images. Lumen is moderately stenosed. * indicates lumen. Original magnification ×10.

artery with a longitudinal coverage of 2 cm each) with different contrast weightings (TOF, T1-, PD-, and T2-weighted) that could be compared with the corresponding histological sections of the endarterectomy specimens. Cohen's κ analysis of lesion type, comparing adjacent locations, was ≤ 0.20 for both forward and backward κ, which indicates that each location could be considered as an independent assessment.

Our patient population with advanced lesions yielded a large number (92/252) of complex plaques (type VI) with surface defects, hemorrhage, and thrombosis. The remaining matched locations consisted of 37 intermediate plaques (type III), 56 atheromatous and fibroatheromatous plaques (type IV-V), and 46 calcified plaques (type VII). Only 12 locations corresponded to type I-II lesions and 9 to type VIII lesions. Figures 1 through 6 show sample images for each lesion type and their corresponding histological sections.

Table 2 summarizes the results of high-resolution MRI and histological examination in the classification of 252 histological slices. The overall correct classification was 80.2% (202/252). None of the advanced lesions (types IV-V, VI, VII, or VIII) were incorrectly classified as early (type I-II) or intermediate (type III) lesions. Overall, the Cohen's κ value between the classification obtained by MRI and the histological classifications (Table 2) was 0.74 (95% CI 0.67 to 0.82), and weighted κ was 0.79, corresponding to good agreement. The sensitivity and specificity, respectively, of MRI for categorizing each lesion type was as follows: type I-II, 67% and 100%; type III, 81% and 98%; type IV-V, 84% and 90%; type VI, 82% and 91%; type VII, 80% and 94%; and type VIII, 56% and 100%.

Discussion

This study provides the first evidence that classification of lesion types based on the appearance of the carotid athero-

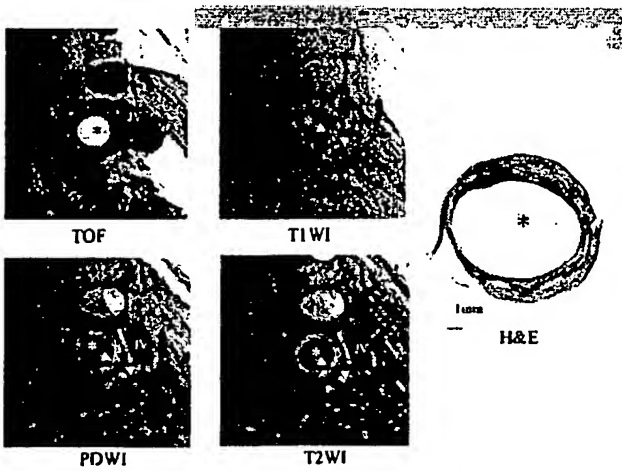

Figure 2. Example of type III lesion in common carotid artery (extracellular lipid pool was detected by histology). On multicontrast-weighted MR images, carotid wall shows slight eccentric thickening (arrow). * indicates lumen; JV, jugular vein; H&E, hematoxylin and eosin. Original magnification ×10.

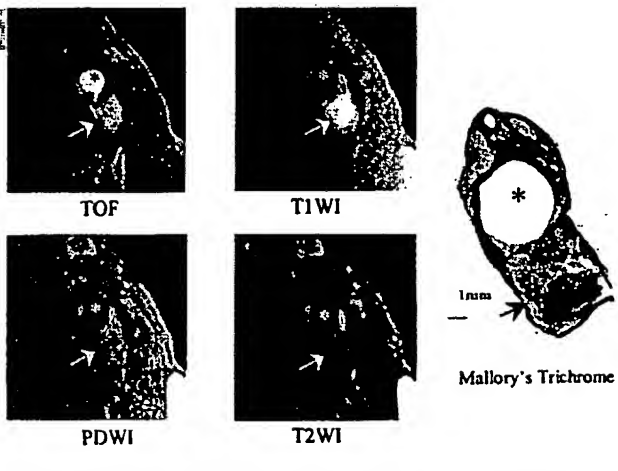

Figure 4. Example of type VI lesion just distal to carotid bifurcation (acute to subacute mixed hemorrhages were detected by histology). On multicontrast-weighted MR images, acute and subacute mixed hemorrhage had high SI on both TOF and T1WI images, iso-SI to slightly high SI on PDWI and T2WI images (arrow). * indicates lumen. Original magnification ×10.

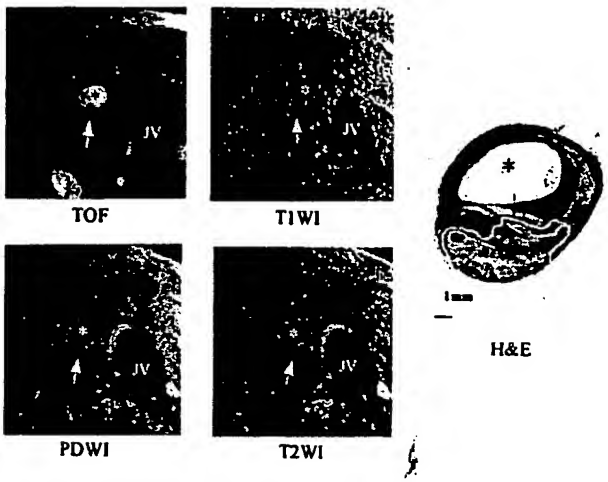

Figure 5. Example of type VII lesion in common carotid artery. Extensive calcification was present in plaque by histology (boundary of calcified region is outlined for clarification.). On multicontrast-weighted MR images, calcified region (arrow) had low SI on all images. * indicates lumen; JV, jugular vein; H&E, hematoxylin and eosin. Original magnification ×10.

sclerotic plaque with in vivo, high-resolution, multicontrast-weighted MRI closely agrees with histological findings according to our slightly modified AHA classification, with a κ-value of 0.74 for the overall agreement. MRI has the potential to document carotid lesion types noninvasively.

In an ex vivo study that was designed to classify atherosclerotic plaques, Serfaty et al[10] showed that ex vivo high-resolution MRI with T2W alone could accurately classify fibrocalcific plaque but was subject to limitations in the classification and analysis of other types of atherosclerotic lesions. Their study did not include preatheromatous lesions (type III) and complicated lesions with surface defect (type VI) because of the lack of appropriate specimens.

In the present study, high sensitivity and specificity were achieved from type III to type VII lesions with enough sample size (type III 37, type IV-V 56, type VI 92, and type VII 46

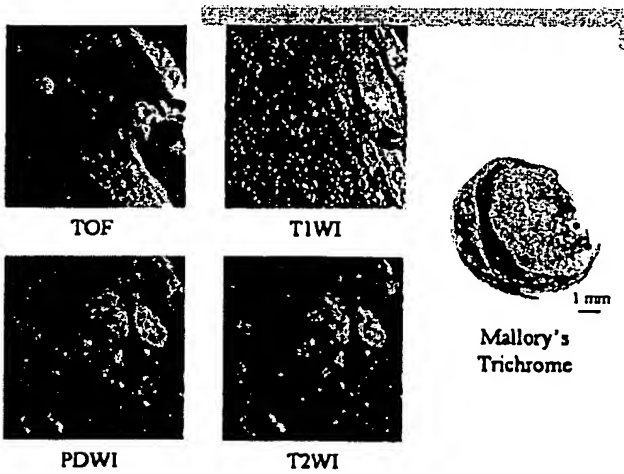

Figure 6. Example of type VIII lesion in internal carotid artery. Connective tissue was characterized by immunocytochemistry as proteoglycan-rich early matrix. Multicontrast-weighted MR images show varied SI. Severely stenosed lumen is marked with asterisk. Original magnification ×10.

TABLE 2. Classification of Carotid Atherosclerotic Plaque by Multicontrast Weighted MRI and Histological Examination

Classification by MRI	Classification by Histological Examination						
	I–II	III	IV–V	VI	VII	VIII	Total
I–II	8	...	...	...	...	...	8
III	4	30	...	...	...	...	34
IV–V	...	7	47	8	2	2	66
VI	...	...	6	75	7	1	89
VII	...	...	3	9	37	1	50
VIII	...	...	...	...	...	5	5
Total	12	37	56	92	46	9	252

Cohen's κ (95% CI)=0.74 (0.67 to 0.82); weighted κ=0.79.

samples) but low sensitivity for type I-II (67%) and type VIII (56%), with 12 and 9 cases, respectively. Results for detecting the lipid-rich necrotic core (type IV-V) and recent hemorrhage (type VI) showed good agreement with previously reported data.[8]

Given the complexity of tissue components, the use of multiple contrast weightings is important for plaque tissue characterization[6–8] and lesion-type classification. In particular, the SI of hemorrhage is dependent on the structure of hemoglobin and its oxidation state.[15] Recent (subacute) hemorrhage with short T1 and long T2 shows a high SI on all contrast-weighted images and is readily identifiable. A source of error in the detection of a small amount of hemorrhage is due to the partial volume effect by which the signal is averaged. We found that this factor alone contributed to the misinterpretation of 8 of 17 false-negative cases in the type VI lesion category. Although calcification is easily detected by MRI on all contrast weightings, calcium on the plaque surface or calcific nodules that extend into the lumen are easily masked on black-blood sequence (spin-echo or fast spin-echo T1, PD-, and T2-weighted)[8] because of low SI; they are easier to detect on bright-blood sequence (TOF). Great care must be taken to examine the surface of type VII lesions (calcific plaque) for irregularities or possible defects. Nine cases with predominant calcification but with a small surface defect were classified incorrectly because the surface appeared smooth on a bright-blood sequence (TOF).

FC is an important structure for the stability of the plaque.[16–19] Falk[16] noted that >75% of major coronary thrombotic events were precipitated by atherosclerotic plaque rupture, which resulted in the exposure of thrombogenic subendothelial plaque constituents. Falk and other researchers[17–19] suggested that plaque disruption and erosion was the critical feature in these moderately stenotic, high-risk lesions. MRI can detect FC status (thick, thin, and ruptured) ex vivo and in vivo.[12,13,20] Hatsukami et al[12] demonstrated that high-resolution MRI with a 3D TOF protocol was capable of distinguishing intact, thick FCs from intact thin and ruptured caps. There was a high level of agreement between MRI and histological findings (89% agreement, κ=0.83). Yuan et al[13] in our group using the same technique demonstrated that MRI identification of a ruptured FC was highly associated with a recent history of transient ischemic attack or stroke.

By the AHA classification,[1,4] the FC may be thin or thick for type IV (atheroma) and type V (fibroatheroma) lesions and may be defective for type VI. Both are advanced atherosclerotic lesions and are clinically relevant. Therefore, in the modified classification in the present study, we used MRI to differentiate ruptured FCs from intact FCs and did not categorize thin or thick FCs within type IV and V lesions, although we can do this with the current technique. In fact, the prognosis of atherosclerotic plaque with thick or thin FCs may be different. In a systematic pathological study with a large number of coronary arteries, Virmani and colleagues[17] proposed a simpler classification based on a descriptive morphology that focuses on the state of the FC. Their classification scheme included 7 categories: intimal xanthoma, intimal thickening, pathological intimal thickening, FC atheroma, thin FC atheroma, calcified nodule, and fibrocalcific plaque. MRI may detect thin FC atheroma and provide more information to the clinician. In the future, a new mixed lesion-type classification of carotid artery based on both histology and MRI may be more practical for the evaluation of patients with carotid atherosclerotic plaque.

Study Limitations

All the MR images were obtained from patients undergoing carotid endarterectomy. Thus, the atherosclerotic lesions in major part of the specimens were advanced. Only 12 locations for type I-II and 9 locations for type VIII lesions were included in this study, and the sensitivity of type I-II and VIII was relatively low. The results should be interpreted with caution. A representative study for these classifications may require scanning more patients with earlier lesions and lesions in different parts of the vascular beds; however, it will be difficult to obtain histological confirmation.

The most pressing concern for the lesion-type classification deals with the resolution of MRI. Although we obtained the best current resolution for in vivo MRI carotid artery study, the resolution was not good enough to detect small structures or components, such as erosion, small surface defect, or small amounts of hemorrhage <0.25 mm in size. Motion artifacts, caused by patient movement or arterial pulsation, also degrade MR image quality. Partial volume effect averages the signal of small components and can cause false-negative results (8 of 17 false-negative cases in the lesion type VI category). Further improvement in coil design, modification of imaging parameters, and faster hardware are needed.

Some new MR technologies have been used in the characterization of carotid atherosclerotic plaque. Shinnar et al[6] and Toussaint et al[21] showed that diffusion-weighted MRI ex vivo was a good technique for identifying thrombus and hemorrhage in plaque. However, there are significant problems in obtaining high-resolution diffusion images of carotid plaque in vivo, because of motion and low signal-to-noise ratio of these imaging techniques. Yu et al[22] noted that a novel fibrin-targeted paramagnetic nanoparticle contrast agent might allow sensitive early detection of unrecognized vascular pathology (thrombus) in high-risk patients. Recently, Yuan et al[9] showed that comparison of pre– and post–contrast-enhanced T1W images might further improve the accuracy of MRI for distinguishing plaque tissue types. In addition, contrast-enhanced MRI may be the only reliable means to detect neovasculature that can contribute to plaque instability.[9,23] These new technologies and new agents will increase our ability to detect the components of the atherosclerotic plaque in vivo and allow us to achieve better classification capabilities.

Our multicontrast imaging protocol has been optimized since this study was undertaken. Specifically, the TI time of the double-inversion recovery T1WI is now set at 330 ms, which provides adequate flow suppression. A multislice double-inversion recovery technique was developed and adapted for T2W and PDW imaging with improved flow suppression and reasonable acquisition time.

Conclusions

We have shown that high-resolution MRI is capable of classifying intermediate to advanced atherosclerotic lesions in the human carotid artery according to a modified AHA classification and is capable of distinguishing advanced lesions from early and intermediate plaques. This study demonstrates that high-resolution MRI can, with a high degree of sensitivity and specificity, detect characteristics of the vulnerable plaque, such as a thin or ruptured FC, a large lipid or necrotic core, and intraplaque hemorrhage. With this new capability of lesion classification, MRI can be used to noninvasively examine the mechanisms of regression and progression of the carotid atherosclerotic plaque.

Acknowledgments

This research was funded by National Institutes of Health grants R01 HL56874 and RO1 HL60213. The authors wish to acknowledge Zachary E. Miller and Williams S. Kerwin for preparing the manuscript and Geraldo Ortiz for his help in acquiring the high-resolution MR images.

References

1. Stary HC, Chandler AB, Dinsmore RE, et al. A definition of advanced types of atherosclerotic lesions and a histological classification of atherosclerosis. *Circulation*. 1995;92:1355–1374.
2. Inzitari D, Eliasziw M, Gates P, et al, for the North American Symptomatic Carotid Endarterectomy Trial Collaborators. The causes and risk of stroke in patients with asymptomatic internal carotid artery stenosis. *N Engl J Med*. 2000;342:1693–1700.
3. Van Dame H, Vivario M, Boniver J, et al. Histologic characterization of carotid plaques. *Cardiovasc Pathol*. 1994;3:9–17.
4. Stary HC. Natural history and histological classification of atherosclerotic lesions. *Arterioscler Thromb Vasc Biol*. 2000;20:1777–1778.
5. Toussaint JF, LaMuraglia GM, Southern JF, et al. Magnetic resonance images lipid, fibrous, calcified, hemorrhagic, and thrombotic components of human atherosclerosis in vivo. *Circulation*. 1996;94:932–938.
6. Shinnar M, Fallon JT, Wehrli S, et al. The diagnostic accuracy of ex vivo MRI for human atherosclerotic plaque characterization. *Arterioscler Thromb Vasc Biol*. 1999;19:2756–2761.
7. Fayad ZA, Fuster V. Characterization of atherosclerotic plaques by magnetic resonance imaging. *Ann N Y Acad Sci*. 2000;902:173–186.
8. Yuan C, Mitsumori LM, Ferguson MS, et al. The in vivo accuracy of multispectral MR imaging for identifying lipid-rich necrotic cores and intraplaque hemorrhage in advanced human carotid plaques. *Circulation*. 2001;104:2051–2056.
9. Yuan C, Kerwin WS, Ferguson MS, et al. Contrast-enhanced high resolution MRI for atherosclerotic carotid artery tissue characterization. *J Magn Reson Imaging*. 2002;15:62–67.
10. Serfaty JM, Chaabane L, Tabib A, et al. Atherosclerotic plaques: classification and characterization with T2-weighted high-spatial-resolution MR imaging—an in vitro study. *Radiology*. 2001;219:403–410.

11. Coombs BD, Rapp JH, Ursell PC, et al. Structure of plaque at carotid bifurcation: high-resolution MRI with histological correlation. *Stroke*. 2001;32:2516–2521.
12. Hatsukami TS, Ross R, Polissar NL, et al. Visualization of fibrous cap thickness and rupture in human atherosclerotic carotid plaque in-vivo with high-resolution magnetic resonance imaging. *Circulation*. 2000;102:959–964.
13. Yuan C, Zhang SX, Polissar NL, et al. Identification of fibrous cap rupture with magnetic resonance imaging is highly associated with recent transient ischemic attack or stroke. *Circulation*. 2002;105:181–185.
14. Fleiss JL. *Statistical Methods for Rates and Proportions*. 2nd ed. New York, NY: John Wiley & Sons; 1981.
15. Bradley WG Jr. MR appearance of hemorrhage in the brain. *Radiology*. 1993;189:15–26.
16. Falk E. Coronary thrombosis: pathogenesis and clinical manifestation. *Am J Cardiol*. 1991;68:28B–35B.
17. Virmani R, Kolodgie FD, Burke AP, et al. Lessons from sudden coronary death: a comprehensive morphological classification scheme for atherosclerotic lesions. *Arterioscler Thromb Vasc Biol*. 2000;20:1262–1275.
18. Carr S, Farb A, Pearce WH, et al. Atherosclerotic plaque rupture in symptomatic carotid artery stenosis. *J Vasc Surg*. 1996;23:755–766.
19. Sitzer M, Muller W, Siebler M, et al. Plaque ulceration and lumen thrombus are the main sources of cerebral microemboli in high-grade internal carotid artery stenosis. *Stroke*. 1995;26:1231–1233.
20. Winn WB, Schmiedl UP, Reichenbach DD, et al. Detection and characterization of atherosclerotic fibrous caps with T2-weighted MR. *Am J Neuroradiol*. 1998;19:129–134.
21. Toussaint JF, Southern JF, Fuster V, et al. Water diffusion properties of human atherosclerosis and thrombosis measured by pulse field gradient nuclear magnetic resonance. *Arterioscler Thromb Vasc Biol*. 1997;17:542–546.
22. Yu X, Song SK, Chen J, et al. High-resolution MRI characterization of human thrombus using a novel fibrin-targeted paramagnetic nanoparticle contrast agent. *Magn Reson Med*. 2000;44:867–872.
23. Aoki S, Aoki K, Ohsawa S, et al. Dynamic MR imaging of the carotid wall. *J Magn Reson Imaging*. 1999;9:420–427.